Photons and photonics in solar cells and photodiodes

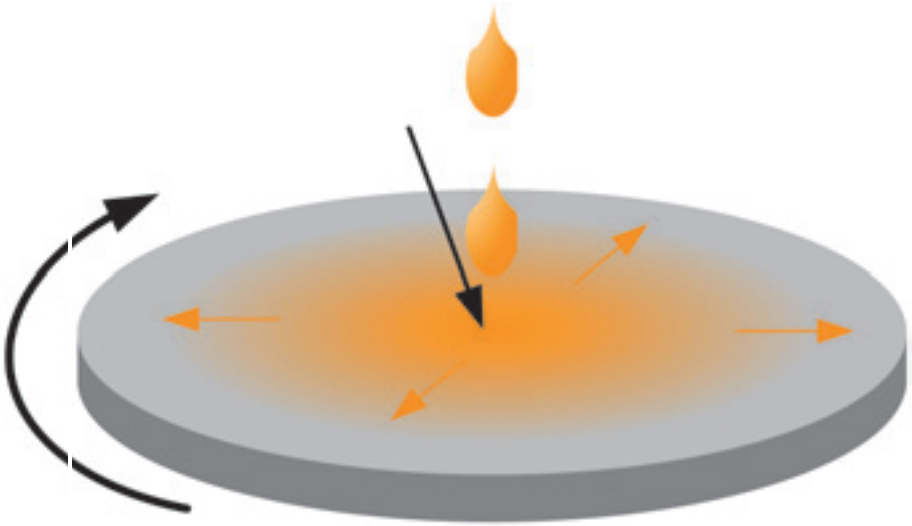

Solar cells and photodiodes rely on the interaction of photons with the electron/hole system of semiconductors. After the absorption of photons, transport of excess electrons and holes results in the observation of an electrical signal at the contacts of the diodes. However, the fabrication of high efficiency solar cells or photodetectors requires far more than the seemingly simply physics and technology of fabricating "just a large area diode". Instead, sophisticated theoretical and practical concepts are necessary for such high efficiency devices.

1. Photovoltaic fluorescent collectors combined with photonic filters

The concept of photonic crystals, three-dimensional periodic dielectric structures that allow for the complete control over the propagation of electromagnetic waves, was introduced by Yablonovitch in 1987 [1]. Since then, photonic crystals entered in a wealth of implementations in opto-electronics, laser optics, and photonics. Surprisingly, photonic crystals have not found any application in photovoltaics up to the present. In fact, the usefulness of this concept for improving solar cells has been disputed even in the original publication [1]. The difficulty to combine photonic crystals with solar cells lies in the fact that photonic crystals can manage electromagnetic waves in an arbitrary, but relatively narrow, range of wavelengths. In contrast, solar cells have to handle the complete band of the solar spectrum. However, the recently reinforced effort to overcome classical limits of photovoltaic power conversion [2] has also brought the use of advanced optical nanostructures (among them: photonic crystals) for solar cells under reconsideration.

Here we briefly sketch a combination of photonic nano-structures with the classical

SUMMARY

This contribution gives three examples for the research on photonics and optoelectronics at the Institute of Physical Electronics (ipe). Part 1 decribes our work on fluorescence converters for solar cells. The combination of these converters with photonic crystals opens a new way to boost the efficiency of classic solar cells. Part 2 presents the application of amorphous silicon photodiodes as large area light sensors in modern digital cameras. The combination of our technology with high dynamic range cameras (HDRC) has the potential of constructing future cameras with a much higher resolution and sensitivity. Finally, part 3 reports on the laser as a tool in the preparation of solar cells. Here, the laser replaces the classic furnace diffusion of a pn-junction. In fact, this process seems to be simple. However, at present we are the only group in the world that is able to fabricate an emitter for a solar cell in a such well defined way with the help of a scanned laser.

concept of fluorescent collectors (FCs). Classical FCs, as already intensely investigated during the 1980s [3,4], use organic dyes or inorganic fluorescent molecules embedded in a dielectric material to collect and concentrate solar light. As sketched in **(01)**, the incoming light is first absorbed by the dye in the collector and then re-emitted at a lower photon energy. This re-emission serves also for the randomization of the light. As a consequence, the classical concentration effect of FCs results from the total internal reflection of the randomized light. However, only photons with a direction outside of the critical angle of internal reflection are kept in the system and the collection efficiency of such a system will be *always* considerably below unity.

(01) also features the possibility to put a photonic band stop (PBS) filter at the top of the collector. This PBS should be designed to be transparent for the incoming light above a certain threshold photon energy E_{th} but should provide a reflectance of unity for those photons that are re-emitted from the dye. In this way, 100% of those photons are kept within the system. Note that practical means to realize PBS with omnidirectional optical reflection in specific wavelength ranges are readily available using technologies that are able to cover large areas, e.g., by one-dimensional periodic dielectric structures [5], i.e., thin film interference filters.

(02) shows the results of a recent Monte-Carlo analysis of the collection properties of FCs with and without PBS [6]. Here we consider the situation where only radiative losses, as required by the principle of detailed balance, are allowed within the FC *and* the solar cells at its bottom. The coverage fraction f is defined by the portion of the FC's backside that is covered by the solar cells. We see that the system *with* a PBS has a maximum efficiency of $\eta = 33\%$ at $f = 1$. Interestingly this maximum equals the maximum conversion efficiency of a solar cell having a band gap energy E_g that equals the threshold energy E_{th} of the FC. Thus, even with PBS, FCs cannot overcome the classical Shockley-Queisser limit [7] for photovoltaic energy conversion. However, almost the same efficiency is maintained at a coverage fraction $f = 0.01$, i.e., with a 99% saving of solar cell material. In contrast, the system *without* PBS has a maximum efficiency of only $\eta = 29\%$ at $f = 1$ due to the losses discussed above. Furthermore, with decreasing f, the available η drops sharply such that any saving of solar cell material has to be paid by losses in output power.

The benefit from the use of photonic band structures for this idealized system is obvious. However, more realistic configurations that include also non-radiative losses in the collector as well as in the solar cells exhibit similar efficiency gains by using the spectral selectivity of photonic band structures [6]. Experimental and technological work is in progress in order to demonstrate this effects also in practical systems.

2. Thin-Film-on-CMOS camera technology

Hydrogenated amorphous silicon (a-Si:H) and its alloys with carbon (a-SiC:H) or germanium (a-SiGe:H) open new possibilities of constructing photodetectors with a superior performance over their crystalline silicon counterparts. Thin film photodiodes greatly enhance the capabilities of modern CMOS (complementary metal oxide semiconduc-

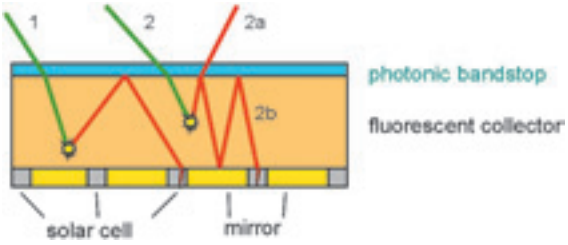

01

Schematic drawing of a fluorescent collector with solar cells at its bottom. The fluorescent layer absorbs incoming photons (1) and emits them at lower photon energy. Without photonic band stop (PBS) some of these photons leave the collector (2a). The PBS reflects these photons back into the collector (2b).

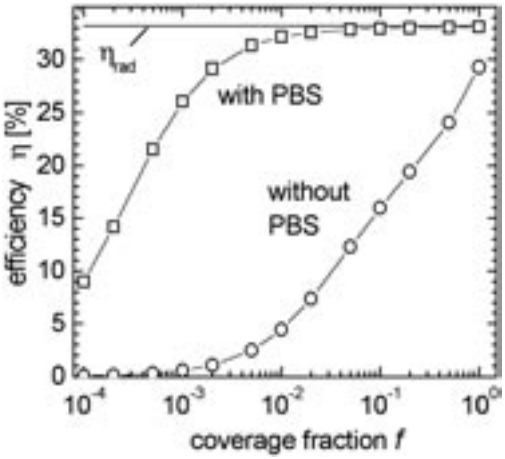

02

Efficiencies for band gap energy Eg = 1.12eV and threshold energy Eth = 1.32eV for ideal solar cells. Without photonic band stop (PBS) the efficiencies degrade rapidly with decreasing coverage fraction f (circles). With PBS the systems efficiency drops much slower with decreasing f (squares) almost maintaining the optimum efficiency down to f = 10-2.

tor) cameras by the so-called "Thin-Film-on-CMOS (TFC)" technology.

Modern CMOS image sensors, also often addressed as "Active Pixel Sensors" (APS), are successfully competing with CCDs (charge-coupled devices) in volume as well as high definition applications [8]. Cost, system integration, and manufacturing issues clearly favour CMOS cameras, whereas CCDs still feature the smallest pixels and ultimate sensitivity. Standard CMOS camera design faces an inherent dilemma: The very same pixel area, which ought to be as small as possible, hosts a diode as photodetector and all readout and signal conditioning circuits at the same time. If sophisticated readout electronics for correlated double sampling, adaptable integration time, or application specific pre-processing is needed, very little space is left for the photodiode. Hence the "eye" of the CMOS camera will be almost blind. On the contrary, photodiodes with a large area fill factor limit the number of transistors inside the pixel, and hence the chance for hardware-based signal processing.

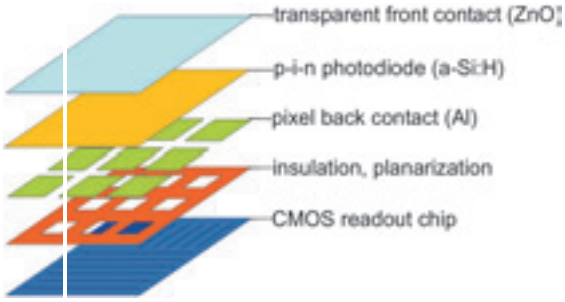

03

Schematic representation of a Thin-Film-on-CMOS layer system. Three-dimensional integration of amorphous silicon based thin film photodiodes enhances the functionality of an underlying CMOS camera chip. Wafer production ends with an open pixel contact in the top metallization layer. After planarization of the interconnect stack and pixel back contact formation, plasma enhanced chemical vapour deposition grows a p-i-n type thin film photodiode which needs no patterning into single pixels. Finally, aluminium doped zinc oxide forms the transparent front contact.

Current and future semiconductor technology lends an additional argument to enhancing CMOS cameras by the three-dimensional addition of a-Si:H based photodiodes. As the standard feature size is shrinking according to Moore's law, *pn*-junctions become very shallow, resulting in a very low and blue-shifted spectral sensitivity. Moreover, interconnect and passivation layers pile up to several micrometers height. The viewing angle of the wafer-based photodiodes consequently shrinks into a "chimney view" through a tiny hole in the interconnect stacks.

04

The impressively high dynamic range of 120 dB in this photograph results from both, a sophisticated logarithmic input stage in the underlying HDRC readout chip, and the six orders of magnitude in light-to-dark conductivity ratio of the a-Si:H based photodiodes on top of the TFC camera. The inset in the lower right corner presents a microscopic top view of one pixel.

Thin-Film-on-CMOS resolves all these limitations, and adds even more benefits to the novel hybrid CMOS camera system [9]. **(03)** sketches the general layout of a TFC camera pixel. The bottom readout and signal processing circuit is manufactured in state-of-the-art CMOS technology, making best use of optimized mixed-signal design and wafer processing. No photodiode is present in the pixel on the wafer, but integrated on top of the interconnect and planarization layers. Manufacturing of the readout electronics provides one top contact per pixel, which later connects to the back contact of the thin film photodiode.

Due to the short diffusion length L_D of charge carriers in the a-Si:H based semiconductors of typically L_D = 100 to 150 nm, no pixel separation is needed in the upper photodiode layers. Down to a back contact spacing of 1.5 µm, the cross-talk between adjacent pixels outperforms CCDs by a factor of 5 to 10. Moreover, the small diffusion length determines the layer structure of the thin film photodiodes. Contrary to crystalline semiconductors, diffusion based carrier collection is almost impossible in these amorphous materials. Therefore a built-in electric field must serve for separating the photogenerated charge carriers. The typical *p-i-n* layer structure of such amorphous silicon based photodiodes mainly consists of an undoped absorber layer sandwiched between very thin doped layers which generate the necessary electric field across the intrinsic *i*-layer. Plasma enhanced chemical vapour deposition (PECVD) of a-Si:H proceeds at low temperature between 100 °C and 150 °C. The thin film photodiodes can therefore easily add upon the CMOS chips after all standard semiconductor processing is finished at a silicon foundry, or at the Institute of Microelectronics Stuttgart (IMS-CHIPS), respectively.

The Thin-Film-on-CMOS technology jointly developed by *ipe* and IMS-CHIPS presents a number of advantages over standard APS or CMOS cameras. The three-dimensional integration of photodiodes on top of the readout electronics implements almost 100 percent area fill factor for the pixel photodiode, and for the underlying electronics as well. Consequently, sensitivity and modulation transfer function of TFC systems clearly outperform those of standard active pixel sensors. Modern CMOS cameras with pixel sizes of a few micrometers are limited to fill area factors below 30 to 40 percent. Amorphous silicon itself adds an additional gain in sensitivity, since its optical bandgap $E_g \approx 1.8$ eV is substantially higher than $E_g = 1.1$ eV of crystalline silicon. Hence the detection limit of TFC cameras is only restricted by leakage due

to back contact patterning and by readout noise, rather than by the thermally generated dark current of standard devices. Our photodiodes present typical values of dark current density j_d as low as $j_d = 10^{-10}$ A/cm².

Many applications ask for a spectral sensitivity which is similar to that of the human eye. Thin film a-Si:H photodiodes perfectly match this requirement. Moreover, the hydrogen content of a-Si:H, layer thicknesses and the alloys a-SiGe:H and a-SiC:H provide easy means of continuously adjusting the spectral response of the TFC photodiodes to various fields of application [10].

Manufacturing of complete TFC camera chips is performed in a close cooperation between IMS-CHIPS and our institute. Customer and application specific requirements control the design of the readout electronics at IMS-CHIPS. The readout characteristics of the photodiode signals can be logarithmic as well as linear, with various options of noise reduction, signal pre-processing etc. Highly miniaturized endoscope camera chips contain pixels as small as 4 x 4 µm² but provide a full color resolution, as it is mandatory for medical applications.

(04) presents an impressive example of high dynamic range imaging. The HDRC camera chip in Thin-Film-on-CMOS technology displays details of the glowing filament, and of the imprint on the light bulb in the very same image frame, with a dynamic range up to 120 dB. Proper readout electronics could enable even higer values, due to the very low dark current of a-Si:H or a-SiC:H photodiodes. Similar logarithmic readout is useful for the control of automated welding or laser cutting machines, and for various automotive applications as well.

Highly sophisticated readout electronics in conjunction with well adapted thin film photodiodes allow for ultimate sensitivity in TFC star sensors. Comparatively large pixel sizes of 20 x 20 µm² accommodate the long focal length of star tracking systems which ensure the precise positioning of every satellite in orbit. Due to their high sensitivity, low power consumption and rather simple system integration, TFC star sensors are now challenging the well established technology of CCD and CMOS-APS based star trackers.

The key to high performance of TFC photodetectors is the interplay between the layout of the thin film photodiode and the input of the pixel amplifier or readout circuitry. Depending on the target application, different photodiode structures are needed. **(05a)** demonstrates significant differences in sensitivity, as measured by the external quantum efficiency of different photodiode structures. The layer sequence with the light entering from the p-side of the pin photodiode performs much better due to the difference in charge carrier transport in a-Si:H based materials. Since their effective electron mobility is a factor of 10 to 100 higher than the respective hole mobility, the collection of electrons succeeds across the whole i-layer thickness whereas hole collection is rather limited to the vicinity of the *p*/*I* interface. Consequently, most photogenerated holes recombine on their way to the p-type back contact of the structure depicted at the bottom of **(05a)**. As expected, hole collection can be slightly improved by raising the readout voltage from V = -2 V to V = -3 V which is however the limit set by the supply voltage of the current CMOS technology.

Some applications, for example incorporating radiation hard readout circuits, enforce the use of a *p*-type back contact, and hence a structure with light unfavorably entering from the *n*-side. For such configurations, **(05b)** evaluates the amount of improvement attainable by careful tuning of the *i*-layer thickness. Due to readout noise considerations, the capacitance of

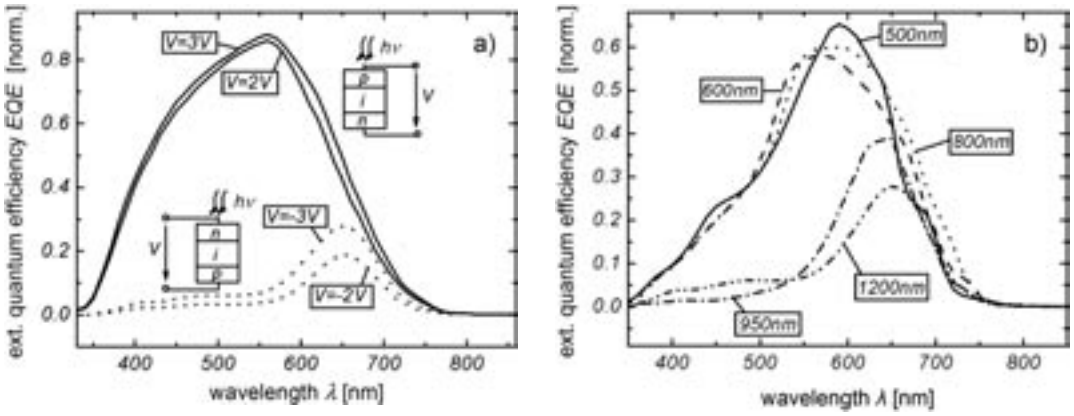

05

(a) *External quantum efficiency* EQE *measurements on comparatively thick TFC diodes reveal the breakdown of charge carrier collection in* n-i-p *structures where the light enters through the* n*-type doped layer. In contrast, the response of* p-i-n *diodes nicely resembles the spectral sensitivity of the human eye, and peaks at values above 80 %. The* i*-layer thicknesses of the* n-i-p *and* p-i-n *diodes amount to 1.2 µm, and 1.5 µm, respectively.* **(b)** *The thickness dependence of* EQE *in* n-i-p *photodiodes proves that an optimum thickness of 700 nm can indeed be used for* n-i-p *TFC layer stacks. Larger* i*-layer thickness clearly hinders hole collection in those structures.*

the thin film photodiode should be as high as possible, asking for thick *i*-layers. **(05b)** demonstrates a significant enhancement of carrier collection if the *i*-layer is kept thin enough to allow for successful extraction of photogenerated holes, and thereby presents a viable compromise in the optimization of sensitivity versus noise reduction. Future applications of TFC technology will further exploit the ease of tuning the spectral response of a-Si:H based thin film photodiodes. **(06)** visualizes the bandgap change by alloying a-Si:H with germanium or carbon. All samples shown have an equal thickness of 1 µm, their colors hence directly indicate the respective optical bandgap E_g. Alloying with Ge enables 1.0 eV < E_g < 1.7 eV, alloying with C raises E_g above 1.8 eV. Reasonable electronic quality can be maintained in a range of 1.4 eV < E_g < 2.1 eV. Interesting applications, e.g. in bioanalytics, arise if the simple *p-i-n* type photodiodes evolve into more sophisticated structures like *n-i-p-i-n* or *p-i-i-n* with varying E_g and layer thickness of the single *i*-layers [10,11]. Such structures open the possibility of dynamically adjusting the spectral response by the variation of the applied readout voltage, and moreover realizing steep gradients of the spectral sensitivity which are useful for discriminating different fluorescence markers or spectroscopic signals in a narrow range of photon energies.

06

Due to the amorphous structure of the a-Si:H based alloys, truly continuous adjustment of the optical bandgap is possible, in contrast to crystalline semiconductors with their well-defined bandgaps. The photograph presents 1 µm thick films with varying alloy composition from a-SiC:H at the left hand side, over a-Si:H in the middle, to a-SiGe:H at the right hand side. Since the film thickness is similar for all films, their color directly visualizes the change in optical bandgap.

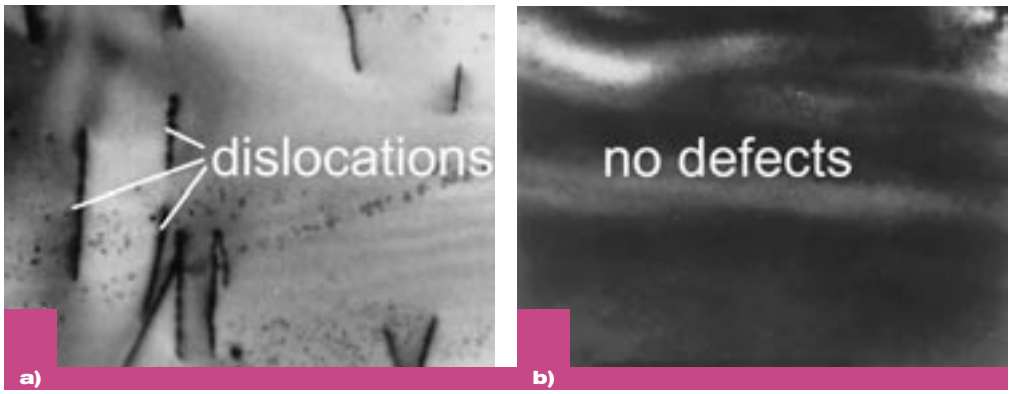

07

Cross section TEM pictures of laser processed silicon wafers. **(a)** *Laser processing with 50 µm circular laser focus results in high defect density.* **(b)** *Line beam shaped laser focus enables recrystallization without any defects.*

3. Room temperature doping of crystalline silicon using pulsed laser radiation

Significant cost reduction in silicon wafer processing for large area electronic devices such as solar cells requires new processing techniques avoiding the most cost intensive steps like wafer handling for batch processing or time and clean room area consuming furnace processing. Our laser doping technology aims at replacing costly high-temperature and vacuum processing steps by low-temperature processing in air.

First papers in the field of laser processing of semiconductors were published in the mid 1970s. Dopant activation of implantation doped silicon and germanium layers was demonstrated for the first time, using laser annealing [12]. Here, the pulse of a Q-switched Nd:glass-laser annealed radiation defects, recrystallized the disordered structure of implantation doped layers, and also stimulated the process of electrical activation of the implanted impurities. Re-crystallization of polycrystalline silicon films on silica and on silicon nitride layers deposited on crystalline silicon wafers also was first achieved using cw-lasers. Yamada et. al. [13] demonstrated the crystallization of sputtered amorphous silicon on sapphire substrates also using a cw-laser. The rapid development of semiconductor laser processing goes hand in hand with the development and availability of new laser sources. Problems with thermal stress cracking of cheap glass substrates during cw-laser crystallization were eliminated by using pulsed lasers, like frequency doubled Nd:YAG and other solid state lasers, as well as gas lasers like excimer-lasers.

More recently, the development and availability of highpower pulsed gas lasers and diode laser pumped solid state lasers with high pulse repetition rates and high average power in the 100 W range made it possible to increase the processing speed and throughput of large area laser processing considerably. The first industrial application of large area laser processing was laser crystallization of amorphous silicon for active matrix liquid crystal displays. Here,

laser processing is performed in air, with a throughput of several 10 cm^2/s.

In contrast to laser crystallization, existing laser doping techniques use vacuum or a protecting atmosphere during irradiation of the samples, which decrease the overall throughput and increase cost. An additional problem of existing laser doping techniques is the high concentration of defects, mainly dislocations, within the recrystallized layer, which leads to a significantly lower open circuit voltage compared to furnace diffusion if laser doping is applied to crystalline silicon solar cells.

Our laser doping process uses a line-beam shaped laser focus with very narrow, below 10 µm, short axis focus. The result is a completely different melting and recrystallization behavior of crystalline silicon compared to laser processing which uses a circular laser focus. The difference between laser crystallization using a circular laser beam focus and a line beam shaped laser beam focus is depicted by the transmission electron microscope images of **(07)**. Our laser processed emitters of monocrystalline silicon solar cells contain no defects. First solar cells processed with this technique achieve open circuit voltages higher than V_{oc} = 620 mV and efficiencies of $\eta > 14\%$ [14]. In fact, the "secret" of our process lies just in the shape of the laser focus on the sample. Without the well-defined shape it would not be possible to obtain large-area, spatially homogeneous pn-junctions with a low saturation current density.

In our experiments, spin coating of phosphorous containing liquid and subsequent drying on a hotplate results in a 400 nm thick solid doping precursor on the surface of a boron doped, *p*-type <100> oriented wafer with thickness $w = 375 \pm 25$ µm and resistivity $\rho = 0.35\ \Omega$cm. **(08)** shows spin coating of a rotating wafer, which leads to a homogeneous distribution of a thin layer of the liquid dopant on the wafer surface.

A lens system consisting of cylindrical and spherical lenses focuses the beam of a 15 ns pulsed frequency doubled Nd:YVO_4 laser onto the surface of the wafer. The laser emits light at a wavelength $\lambda = 532$ nm with a tunable repetition frequency $f <$ 100 kHz and power $P < 1$ W. The size of the line beam shaped laser focus is 5 µm wide in y-direction and 200 µm in the perpendicular x-direction. The intensity distribution is Gaussian in both x and y directions. An automatic focusing system controls the focus size and keeps the pulse energy density at a constant value during wafer processing. An *xy*-translation stage fixes and moves the wafer in *y*-direction with a scanning speed v_y. After each laser pulse the sample is translated by a distance $\Delta y = v_y / f$. We tune the repetition frequency f according to the scanning speed v_y to obtain a translation 0.3 µm $< \Delta y <$ 3 µm, which corresponds to an overlap $95\% > O_y > 40\%$ between the laser pulses. The next column of pulses is then shifted by a distance Δx with respect to the previous column. **(09)** schematically displays the principle of the scanning process. The laser beam scans the surface and creates the emitter by locally melting the silicon and allowing the dopant to diffuse into the wafer. We process different samples varying the energy density D_{pulse} of the laser pulses, the overlap O_x in x- and O_y in y-direction between the pulses.

ZUSAMMENFASSUNG

Die Wirkung von Solarzellen und Photodioden beruht auf der Wechselwirkung von Licht, der Photonen, mit dem elektronischen System, den Elektronen und Löchern eines Halbleiters. Nach der Absorption der Photonen führt der Transport von Elektronen und Löchern zu einem elektrischen Signal an den Kontakten dieser Bauelemente. Für die Herstellung von hocheffizienten Solarzellen und Photodioden benötigt man jedoch bei weitem mehr als die scheinbar einfache Physik und Technologie einer Diode, die 'halt ein bisschen größer ist als üblicherweise'. Die Herausforderung besteht darin, komplexe Konzepte und Technologien zu entwickeln, die zuverlässig und reproduzierbar zu hochwertigen, großflächigen Bauelementen führen.

Dieser Beitrag stellt drei Beispiele der Forschung am Institut für Physikalische Elektronik (ipe) im Bereiche der Photonik und Optoelektronik vor. Teil 1 beschreibt unsere Arbeiten an Fluoreszenzkonvertern für photovoltaische Anwendungen. Die Kombination dieser Konverter mit nano-optischen Strukturen (z.B. photonischen Kristallen) eröffnet neue Möglichkeiten, Licht einfach und effizient zu konzentrieren und somit Solarzellenmaterial zu sparen. Teil 2 demonstriert die Anwendung von amorphem Silizium für großflächige Photodetektoren in modernen digitalen Kameras. Die Kombination unserer Technologie mit so genannten high dynamic range cameras (HDRC) erlaubt in Zukunft die Herstellung von Kameras mit einer viel größeren Auflösung und Empfindlichkeit. Schließlich berichtet Teil 3 über die Verwendung von Lasern für die Dotierung von Solarzellen. Mit dieser Technologie kann die energieaufwändige Diffusion eines pn-Übergangs durch einen schnellen, energie- und kosteneffizienten Prozess ersetzt werden. Obwohl die Idee einfach klingt, sind wir derzeit die einzige Forschungsgruppe in der Welt, die diesen Prozess reproduzierbar und auf hohem Niveau beherrscht.

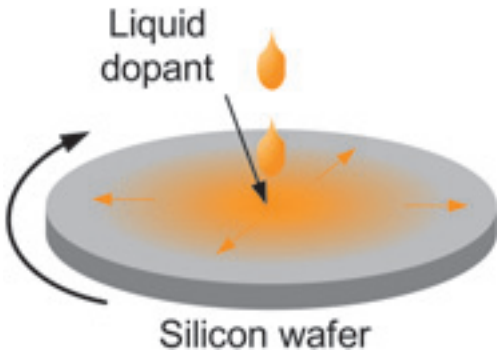

08

Spin coating covers the silicon wafer with a thin layer of a dopant containing liquid.

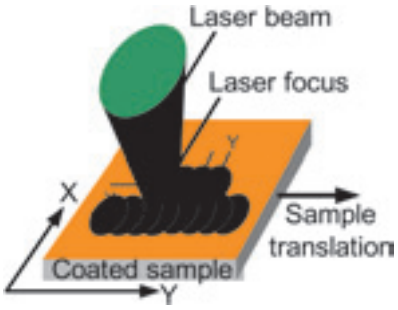

09

Sketch of the LD process. Each pulse melts a several hundred nanometer thick layer of silicon under the phosphorous containing paste and phosphorous atoms diffuse into the molten layer. The laser scans the wafer with a shift 0.3 µm < Dy < 3 µm in Δy-direction and 100 µm < Dx < 200 µm in Δx-direction between the laser pulses.

10

Finished solar cell with antireflection layer and contacts.

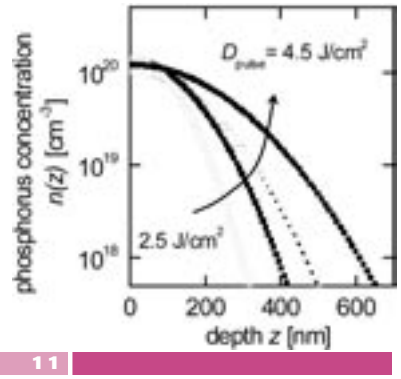

11

Phosphorus depth profile measured by SIMS of four solar cells processed with pulse energy densities D_{pulse} = 2.5, 3.2, 3.8 and 4.5 J/cm². The effective depth z of the emitter increases with the pulse energy density D_{pulse}.

After laser processing of the samples, the front contacts are formed by vacuum evaporation of 2 µm thick Ti/Pd/Ag fingers using a mask. The back contact consists of an evaporated 1.5 µm thick aluminum layer. A 75 nm thick SiN_x layer with a refractive index n_r = 1.9 additionally serves as anti-reflection layer. Contacts are annealed in forming gas at 420 °C for 10 minutes in order to improve the electronic contact properties. Finally a mesa structure is formed by CF_4 plasma-etching to define the cell area. **(10)** depicts the completion of the solar cell by adding an antireflective coating as well as front and back contacts.

We use different analyzing techniques to investigate the influence of the laser doping process on the performance of the solar cells. Secondary ion mass spectroscopy determines the depth and lateral distribution of the dopant concentration. **(11)** shows the phosphorous depth profile of four cells processed with pulse energy densities D_{pulse} = 2.5, 3.2, 3.8 and 4.5 J/cm². The LD process creates a shallow highly doped emitter. The emitter depth increases with the pulse energy density D_{pulse}.

(T.01) shows the parameters of a solar cell under 100mW/cm² intensity AM1.5 irradiation, independently confirmed by FhG-ISE, Freiburg. This solar cell is irradiated with a pulse energy density D_{pulse} = 2.5 J/cm², shifted by Δx = 100 µm in x- and Δy = 0.5 µm in y-direction.

J_{sc} [mA/cm²]	V_{oc} [mV]	*FF* [%]	η [%]
31.07	612.3	74.6	14.2

(T.01): Photovoltaic output parameters short circuit current density J_{sc}, open circuit voltage V_{oc}, fill factor *FF*, and efficiency η under 100mW/cm² intensity AM1.5 irradiation. The data are independently confirmed by FhG-ISE, Freiburg. During laser processing, the cell is irradiated with a pulse energy density D_{pulse} = 2.5 J/cm², shifted by Δx = 100 µm in x- and Δy = 0.5 µm in y-direction.

The laser doping process offers a simple manufacturing method of solar cells where diffusion in a clean room environment is superfluous. Solar cells made with the method described above show a high efficiency of η = 14.2% even without photolithographic steps or texture on the front side. At present we study several simplifications of the laser doping process and investigate scaling up to the size of industrial solar cells of 15 x 15 cm². If that stage is reached, the process will be transferred into an industrial environment of solar cell production.

Jürgen R. Köhler
Uwe Rau
Markus B. Schubert
Jürgen H. Werner

References

1 E. Yablonovitch, Phys. Rev. Lett. **58**, 2059 (1987).
2 M. A. Green, Progr. Photov.: Res. Appl. **9**, 123 (2001).
3 E. Yablonovitch, J. Opt. Soc. Am. **70**, 1362 (1980).
4 A. Goetzberger and V. Wittwer, Solar Cells **4**, 3 (1988).
5 D. N. Chigrin and C. M. Sotomayor Torres, Optics and Spectroscopy **91**, 484 (2001).
6 G. C. Glaeser, F. Einsele, and U. Rau, in *Techn. Digest 15th Photovoltaic Science and Engineering Conference* (in print).
7 W. Shockley and H. J. Queisser, J. Appl. Phys. **32**, 510 (1961).
8 E. Fossum, IEEE Transact. Electron Devices **44**, 1689 (1997).
9 H. Fischer, J. Schulte, J. Giehl, M. Böhm, and J. P. M. Schmitt, Mat. Res. Soc. Symp. Proc. **258**, 1139 (1992).
10 K. Eberhardt, T. Neidlinger, and M. B. Schubert, IEEE Trans. Electron. Dev. **ED-42**, 1763 (1995).
11 R. Brüggemann, T. Neidlinger, and M. B. Schubert, J. Appl. Phys. **81**, 7666 (1997).
12 E. I. Shtyrkov, I. B. Khaibullin, M. M. Zarpov, M. F. Galyatudinov, and R. M. Bayazitov, Sov. Phys. Semicond. **9**, 1309 (1975).
13 M. Yamada, S. Hara, K. Yamamoto, and K. Abe, Jpn. J. Appl. Phys. **19**, 261 (1980).
14 A. Esturo-Breton, T. A. Wagner, J. R. Köhler, and J. H. Werner, in *13th Workshop on Crystalline Silicon Solar Cell Materials and Processes*, edited by B. Sopori (NREL, Golden CO, 2003), p. 186.

THE AUTHORS

JÜRGEN KÖHLER

studied Physics in Tübingen and Stuttgart. During his diploma thesis in 1984 he worked at the Institut für Physikalische Elektronik (ipe), faculty of electrical engineering, on optical spectroscopy of molecules in high pressure gases. Between 1985 and 1990 he worked at ipe in the frame of several R&D projects in the field of laser spectroscopy and material processing and towards his Ph. D. thesis. In 1990 he became the head of the research group "applied laser and measurement techniques", where he was responsible for several EC, BMBF and bilateral industrial R&D projects. In 1991 he became member of the permanent scientific staff at ipe. He obtained his Ph. D. from the Universität Stuttgart in 1996. Since 1997, he is heading the laser-processing research group at ipe.

UWE RAU

received the Ph. D. degree in physics in 1991 from the University of Tübingen, Germany, for his work on temporal and spatial structure formation in the low-temperature electronic transport of bulk semiconductors. From 1991–1994 he worked at the Max-Planck-Institut für Festkörperforschung, Stuttgart, Germany, in the field of Schottky contacts, semiconductor heterojunctions and silicon solar cells. From 1994–1997 he was with the University of Bayreuth, Germany, working on electrical characterization and simulation of silicon and CuInSe2 solar cells. In 1997 he joined the Institut für Physikalische Elektronik at the Universität Stuttgart, where he became leader of the device analysis group. In 2002, he received the habilitation from the Carl-von-Ossietzky Universität Oldenburg. His research interest are electronic, ionic, and photonic transport in solar cells, as well as interface and bulk defects in semiconductors.

MARKUS B. SCHUBERT

holds a Dipl.-Ing. and a Dr.-Ing. degree, both obtained from the Faculty of Electrical Engineering at the Universität Stuttgart. Since 1985, he worked as a research assistant at Stuttgart University, Institute of Physical Electronics (ipe). Since 1993 he serves as a group leader at ipe, managing various research projects on thin film sensors and solar cells. M. B. Schubert has authored and coauthored more than 100 publications. Since 1999, he assists Prof. J. H. Werner as the associate director of ipe.

JÜRGEN H. WERNER

studied Physics in Tübingen and received the Ph.D. degree in Physics in 1983 from the Universität Stuttgart. The PhD thesis on polycrystalline silicon was carried out at the Max-Planck-Institut für Festkörperforschung, Stuttgart. After working as a scientist at the Max-Planck-Institut, he spent 18 months in the USA as a guest scientist at the IBM T. J. Watson Research Center, Yorktown Heights, N.Y., USA at AT&T Bell Laboratories, Murry Hill, N. J., USA working on Schottky diodes. In 1991, Jürgen Werner received the habilitation from the University of Munich. In these years, his research concentrated on semiconductor interfaces. In 1996 he became the director of the Institute for Physical Electronics (ipe) in 1996, where he has been teaching and researching since then in the field or micro- and optoelectronics. The research emphasis of the ipe is placed on photodectors, solar cells and solar cell materials. Jürgen H. Werner is author and co-author of over 215 publications and the editor of nine books.

Contact

Institut für Physikalische Elektronik, Universität Stuttgart, Pfaffenwaldring 47, 70569 Stuttgart
Tel. +49 (0)711 6857141
Fax +49 (0)711 685 7143
E-mail: sekretariat@ipe.uni-stuttgart.de

zurück zum Inhalt